

The Synthesis of Single-Crystalline BaFe₁₂O₁₉ Nanoparticles by Molten-Salt Method with Surfactant NP-9

Xueyong Yuan · Kai Shen · Mingxiang Xu · Qingyu Xu

Received: 19 April 2012 / Accepted: 8 May 2012 / Published online: 25 May 2012
© Springer Science+Business Media, LLC 2012

Abstract Single-crystalline barium ferrite (BaFe₁₂O₁₉) nanoparticles have been successfully synthesized by the molten-salt method. The particles of both samples with and without surfactant NP-9 possess hexagonal plate-like shape. However, BaFe₁₂O₁₉ nanoparticles without NP-9 during the preparation exhibit two different magnetic phases (soft and hard) reflected from the double magnetic hysteresis loops, and the soft magnetic phase was attributed to the defect region in the nanoparticles. Including the surfactant NP-9 in the preparation process, the soft magnetic phase was effectively suppressed, and only the hard magnetic phase was observed, reflected from the single magnetic hysteresis loop. Furthermore, the remanent magnetization and saturate magnetization were increased slightly by using NP-9. These results indicate that NP-9 is an effective additive for the preparation of high-quality single-crystalline ferrite nanoparticles.

Keywords BaFe₁₂O₁₉ · Molten-salt method · Surfactant

1 Introduction

M-type barium ferrite with hexagonal molecular (BaFe₁₂O₁₉) has aroused considerable interest in the magnetic material field due to its fairly large magnetocrystalline anisotropy, high Curie temperature, relatively large magnetization, excellent chemical stability and corrosion resistivity [1–3]. So far, various techniques have been proposed for the synthesis of BaFe₁₂O₁₉ and these mainly include the conventional ceramic process of solid-state reaction [4], co-precipitation/hydrothermal synthesis [5], sol–gel progress [6], molten-salt method [7], etc.

The molten-salt method has several advantages over the conventional solid-state reaction and sol–gel methods. The reaction temperature of the molten-salt method (800–1000 °C) is much lower than the conventional solid-state reaction method (1200–1350 °C) and much less reaction time (1–2 h) than the sol–gel method (4–5 h) [7]. Furthermore, the molten-salt method shows good control of particle morphology. For example, by the conventional solid-state reaction method, the hexagonal platelets of homogeneous composition and uniform particle distribution are very difficult to form [8]. Well shaped hexagonal platelets of Sr-ferrites and Ba-ferrites nanoparticles have been successfully fabricated by the molten-salt method [7, 8]. However, the size distribution is still rather nonuniform [7, 8]. Surfactant NP-9 has been successfully used in the preparation of the BiFeO₃ and Bi₂Fe₄O₉ nanoparticles by molten-salt method, and well cubic shaped BiFeO₃–BaTiO₃ and Bi₂Fe₄O₉ nanoparticles with uniform size distribution have been successfully fabricated [9, 10]. In this paper, we adopt the successful experience of using NP-9 in the molten-salt method to prepare the BaFe₁₂O₁₉ nanoparticles. Better crystallinity with larger particle size has been obtained, which leads to the improved magnetic properties.

X. Yuan · M. Xu · Q. Xu (✉)

Department of Physics, Southeast University, Nanjing 211189, China
e-mail: xuqingyu@seu.edu.cn

K. Shen

School of Materials Science and Technology, Nanjing University of Aeronautics and Astronautics, Nanjing 210016, China

Q. Xu

Key Laboratory of MEMS of the Ministry of Education, Southeast University, Nanjing 210096, China

2 Experimental Details

The $\text{BaFe}_{12}\text{O}_{19}$ nanoparticles were prepared using sol–gel technique followed by a molten-salt method. First a gel precursor was prepared using sol–gel technique. Stoichiometric amount of $\text{Fe}(\text{NO}_3)_3 \cdot 9\text{H}_2\text{O}$ was dissolved in deionized water and quantitatively precipitated by ammonia solution. The precipitate was washed with deionized water until neutrality, then dissolved in citric acid solution with water bath at 60°C . Since it will generate impurity phase of Fe_2O_3 if we choose the $\text{Fe}/\text{Ba} = 12$, after a series experiments with different Fe/Ba ratios, we choose the $\text{Fe}/\text{Ba} = 11$, which is in agreement with other reports [11]. According to the $\text{Fe}/\text{Ba} = 11$ ratio, a suitable amount of BaCO_3 was added to the mixed solution, which was then stirred for certain time until a transparent solution was achieved. Served as agents, a quantity of ethylene glycol was also added. The solution was slowly evaporated at $60\text{--}80^\circ\text{C}$ and roasted at 120°C until a gel formed. Second, the gel was pre-sintered at 450°C for 4 h. After the pre-sintered intermediate product cooled down, it was mixed with NaCl with weight of 1:10, grinded in agate mortar after the NP-9 was subsequently added. In the synthesis of $\text{BaFe}_{12}\text{O}_{19}$, the ratio was selected as 1 mmol of BaCO_3 with 2 ml NP-9. The choice of NP-9 surfactant was governed by its proven versatility in the preparation of various metal oxide system, as well as its comparative facility of use [9, 10, 12]. These mixed powders were put in alumina crucible, sintered at 1100°C for 2 h. The final product was washed with distilled water and ethyl alcohol and dried in the air. For comparison, $\text{BaFe}_{12}\text{O}_{19}$ nanoparticles were prepared by molten salt without adding NP-9 and by conventional sol–gel method with both sintering temperature of 1100°C .

The structure was analyzed by X-ray diffraction (XRD) using $\text{Cu K}\alpha$. The microstructure and morphology was investigated by a transmission electron microscope (TEM, FEI Techni-S20). The magnetic properties were measured at room temperature using a Physical Property Measurement System (PPMS-9, Quantum Design).

3 Results and Discussion

Figure 1 shows the TEM images of $\text{BaFe}_{12}\text{O}_{19}$ powders synthesized by the sol–gel method and molten-salt method. It is obvious that the particles synthesized by the conventional sol–gel method are very irregular-shaped with much smaller size and the size distribution is rather nonuniform. It can be seen from the graphs that $\text{BaFe}_{12}\text{O}_{19}$ nanoparticles synthesized by molten-salt method show nanorods and platelet-like nanostructures. By adding NP-9 during the sample preparation, the hexagonal platelet-like particles dominate in the products. Furthermore, it is evident that not only the size of

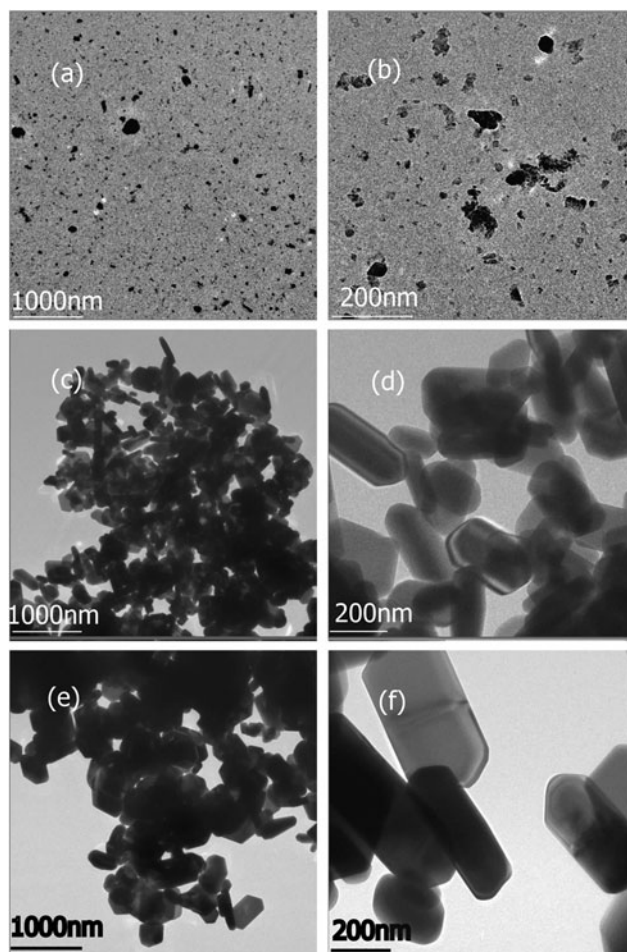


Fig. 1 TEM images of $\text{BaFe}_{12}\text{O}_{19}$ particles synthesized under different conditions: (a) and (b) sol–gel method; (c) and (d) molten-salt method without NP-9; (e) and (f) molten-salt method with NP-9

the particles prepared without NP-9 is smaller, but also the size distribution is far more dispersed.

In order to analyze the phase structure of barium ferrites, XRD analysis was performed, and the patterns are shown in Fig. 2. All peaks of the powders can be indexed as hexagonal $\text{BaFe}_{12}\text{O}_{19}$ (PDF#84-0757). The calculated lattice constant a and c from XRD patterns using the Bragg equation are show in Table 1. Compared with the reference value of $\text{BaFe}_{12}\text{O}_{19}$ (PDF#84-0757), $a = 5.892 \text{ \AA}$, $c = 23.183 \text{ \AA}$, it is clear that only the c lattice constant of $\text{BaFe}_{12}\text{O}_{19}$ synthesized by sol–gel method deviates significantly. Furthermore, it is clear that the signal-to-noise ratio of $\text{BaFe}_{12}\text{O}_{19}$ synthesized by molten-salt method is significantly improved. Thus we can conclude that the $\text{BaFe}_{12}\text{O}_{19}$ nanoparticles synthesized by molten-salt method have better crystallization.

Figure 3 shows magnetic hysteresis loops for the $\text{BaFe}_{12}\text{O}_{19}$ synthesized under different conditions. As shown in the Fig. 3, $\text{BaFe}_{12}\text{O}_{19}$ synthesized with molten-salt method possesses much higher coercivity. It can be seen in Table 2 that the coercivity of $\text{BaFe}_{12}\text{O}_{19}$ prepared by sol–gel method

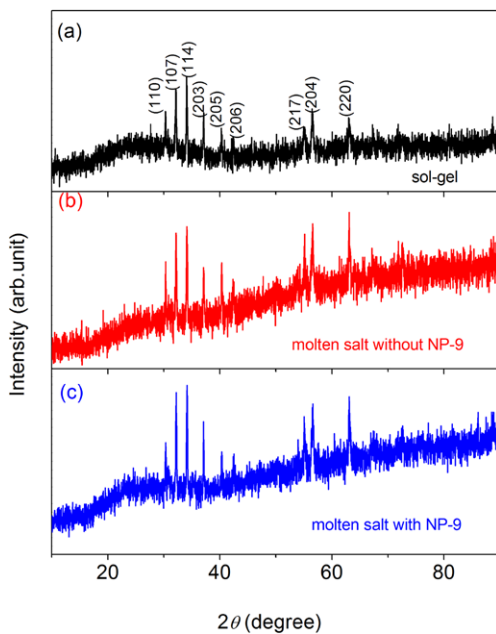


Fig. 2 XRD patterns of BaFe₁₂O₁₉ particles synthesized under different conditions: (a) sol–gel method; (b) molten-salt method without NP-9; (c) molten-salt method with NP-9

Table 1 Calculated lattice constant *a* and *c* from XRD patterns of BaFe₁₂O₁₉ prepared under different conditions

	Sol-gel	Molten salt without NP-9	Molten salt with NP-9	Reference value (JCPDS 84-0757)
<i>a</i> (Å)	5.885	5.892	5.886	5.892
<i>c</i> (Å)	23.217	23.194	23.190	23.195

is 2538 Oe, while BaFe₁₂O₁₉ synthesized with molten-salt method and with NP-9 addition are 4478 Oe and 4121 Oe, respectively. The BaFe₁₂O₁₉ grains synthesized by sol–gel method appear to stick each other and agglomerate in different masses, the shape of grain is irregular. The molten-salt method can improve the grain growth of barium ferrite with better crystallinity, leading to the larger coercivity [7]. However, though the addition of NP-9 further improves the grain growth, the slight decrease of the coercivity might be due to the multi-domain formation and the easy movement of the domain walls [7].

Furthermore, the *M*–*H* loops of both the BaFe₁₂O₁₉ synthesized by sol–gel method and molten-salt method without NP-9 shown in Fig. 3 display a characteristic shrinking at low field, which looks like double hysteresis loops. The magnetic switching behavior can be indicated as the presence of two different “magnetic phases”, one with large *H_c* (hard) and the other with small *H_c* (soft). Interestingly, by using NP-9, there is only single magnetic hysteresis loop with large coercivity, indicating the efficient suppression of the soft magnetic phase. The soft magnetic phase

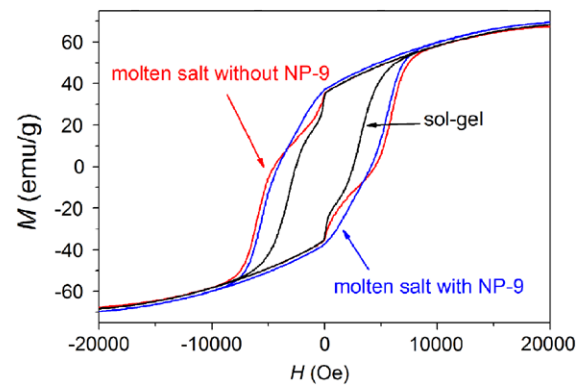


Fig. 3 *M*–*H* loops for the BaFe₁₂O₁₉ prepared under different conditions

may be attributed to the defect regions in the nanoparticles [13]. The NP-9 molecule has both hydrophilic end and lipophilic end [14], which means the addition of surfactant NP-9 would decrease the viscosity of the molten salt [15]. Moreover, the presence of surfactant NP-9 may prevent the interparticle aggregation by forming a ‘shell’ around individual particles [16]. In this case, the BaFe₁₂O₁₉ molecules have more probability to form perfect hexagonal crystal, which contains less defect regions. So the soft magnetic phase was suppressed.

We have determined the remanent magnetization (*M_r*), saturation magnetization (*M_s*) (measured at magnetic field of 20 kOe) and coercivity from the *M*–*H* curves, and were summarized in Table 2. As can be seen, the BaFe₁₂O₁₉ synthesized by molten-salt method with NP-9 has the highest saturate magnetization of 69.5 emu/g, which is close to the theoretically estimated value of 72 emu/g. It is known that the specific saturation magnetization belongs to the intrinsic property for magnetic, which is decided by the components and the structure of materials. It is suggested that the presence of salt is expected to decrease the melt viscosity and thereby the mobility of the components within the molten flux, which will lead to the better growth of the grains and larger grain size compared with the BaFe₁₂O₁₉ nanoparticles by sol–gel method [10]. The presence of surfactant may prevent interparticle aggregation by forming a ‘shell’ around individual particles [10], thus the finer precursor particles might facilitate the ion diffusion in the molten salt. Thus by using NP-9 the BaFe₁₂O₁₉ nanoparticles will have more uniform distribution of ingredients and less defects, leading to the suppression of the soft magnetic phase and increase of the saturate magnetization.

4 Conclusions

Single-crystalline barium ferrite (BaFe₁₂O₁₉) nanoparticles have been successfully synthesized by the molten-

Table 2 Magnetic properties of BaFe₁₂O₁₉ prepared under different conditions

	H_c (Oe)	M_r (emu/g)	M_s (at 20 kOe)	M_r/M_s
Sol-gel	2538	34.0	68.3	0.50
Molten salt without NP-9	4478	35.1	67.5	0.52
Molten salt with NP-9	4121	37.2	69.5	0.54

salt method. The particles of both samples with and without surfactant NP-9 possess hexagonal plate-like shape. However, BaFe₁₂O₁₉ nanoparticles without NP-9 during the preparation exhibits soft and hard magnetic phases reflected from the double magnetic hysteresis loops. Including the surfactant NP-9 in the preparation, the soft magnetic phase was effectively suppressed, and only the hard magnetic phase was observed reflected from the single magnetic hysteresis loop, indicating the suppression of the defects region in the BaFe₁₂O₁₉ nanoparticles. Furthermore, the remanent magnetization, saturate magnetization were increased slightly by using NP-9. These results indicate that NP-9 is an effective additive for preparation of high-quality single-crystalline ferrite nanoparticles.

Acknowledgements This work is supported by the National Natural Science Foundation of China (51172044), the National Science Foundation of Jiangsu Province of China (BK2011617), National Key Projects for Basic Researches of China (2010CB923404), by NCET-09-0296, the Scientific Research Foundation for the Returned Overseas Chinese Scholars, State Education Ministry, and Southeast University (the Excellent Young Teachers Program and Seujq201106).

References

1. Wohlfarth, E.P.: Ferromagnetic Materials. North-Holland, Amsterdam (1982)
2. Pillai, V., Kumar, P., Multani, M.S., Shah, D.O.: Colloids Surf. A, Physicochem. Eng. Asp. **80**, 69 (1993)
3. Wang, S., Ng, W.K., Ding, J.: Scr. Mater. **42**, 861 (2000)
4. Harberer, F., Kockel, A.: IEEE Trans. Magn. **12**, 983 (1976)
5. Haneda, K., Miyakawa, C., Kojima, H.: J. Am. Ceram. Soc. **57**, 354 (1974)
6. Fortes, S.S., Duque, J.G.S., Macedo, M.A.: Physica B **384**, 88 (2006)
7. Yu, J., Tang, S., Zhai, L., Shi, Y., Du, Y.: Physica B **404**, 4253 (2009)
8. Kim, S., Kim, J.: J. Magn. Magn. Mater. **307**, 295 (2006)
9. Park, T., Papaefthymiou, G.C., Viescas, A.J., Lee, Y., Zhou, H., Wong, S.S.: Phys. Rev. B **82**, 024431 (2010)
10. Park, T., Papaefthymiou, G.C., Moodenbaugh, A.R., Mao, Y., Wong, S.S.: J. Mater. Chem. **15**, 2099 (2005)
11. Wang, L., Zhang, Q.: J. Alloys Compd. **469**, 251 (2009)
12. Park, T.J., Wong, S.S.: Chem. Mater. **18**, 5289 (2006)
13. Jin, C., Liu, H., Kuang, D.F., Bai, H.L.: J. Appl. Phys. **110**, 013917 (2011)
14. Lee, S., Teng, M.: Diam. Relat. Mater. **20**, 183 (2011)
15. He, K., Xu, C.Y., Zhen, L., Shao, W.Z.: Mater. Lett. **62**, 739 (2008)
16. Li, L., Wang, W.: Solid State Commun. **127**, 639 (2003)